

PRIMARY RESEARCH

Open Access



# Ferroptosis-related gene signature predicts the prognosis of papillary thyroid carcinoma

Jinyuan Shi<sup>1</sup>, Pu Wu<sup>1</sup>, Lei Sheng<sup>2</sup>, Wei Sun<sup>1</sup> and Hao Zhang<sup>1\*</sup>

## Abstract

**Background:** Papillary thyroid carcinoma (PTC) is the most common type of thyroid cancer (TC), accounting for more than 80% of all cases. Ferroptosis is a novel iron-dependent and Reactive oxygen species (ROS) reliant type of cell death which is distinct from the apoptosis, necroptosis and pyroptosis. Considerable studies have demonstrated that ferroptosis is involved in the biological process of various cancers. However, the role of ferroptosis in PTC remains unclear. This study aims at exploring the expression of ferroptosis-related genes (FRG) and their prognostic values in PTC.

**Methods:** A ferroptosis-related gene signature was constructed using lasso regression analysis through the PTC datasets of the Cancer Genome Atlas (TCGA). Gene Ontology (GO) and Kyoto Encyclopedia of Genes and Genomes (KEGG) enrichment analyses were performed to investigate the bioinformatics functions of significantly different genes (SDG) of ferroptosis. Additionally, the correlations of ferroptosis and immune cells were assessed through the single-sample gene set enrichment analysis (ssGSEA) and CIBERSORT database. Finally, SDG were test in clinical PTC specimens and normal thyroid tissues.

**Results:** LASSO regression model was utilized to establish a novel FRG signature with 10 genes (ANGPTL7, CDKN2A, DPP4, DRD4, ISCU, PGD, SRXN1, TF, TFRC, TXNRD1) to predicts the prognosis of PTC, and the patients were separated into high-risk and low-risk groups by the risk score. The high-risk group had poorer survival than the low-risk group ( $p < 0.001$ ). Receiver operating characteristic (ROC) curve analysis confirmed the signature's predictive capacity. Multi-variate regression analysis identified the prognostic signature-based risk score was an independent prognostic indicator for PTC. The functional roles of the DEGs in the TCGA PTC cohort were explored using GO enrichment and KEGG pathway analyses. Immune related analysis demonstrated that the most types of immune cells and immunological function in the high-risk group were significant different with those in the low-risk group. Quantitative Real-Time Polymerase Chain Reaction (qRT-PCR) verified the SDG have differences in expression between tumor tissue and normal thyroid tissue. In addition, cell experiments were conducted to observe the changes in cell morphology and expression of signature's genes with the influence of ferroptosis induced by sorafenib.

**Conclusions:** We identified differently expressed FRG that may involve in PTC. A ferroptosis-related gene signature has significant values in predicting the patients' prognoses and targeting ferroptosis may be an alternative for PTC's therapy.

**Keywords:** Papillary thyroid carcinoma, Ferroptosis genes, Gene signature, Prognosis, TCGA

## Introduction:

Thyroid cancer (TC) is the most common malignant endocrine tumor and its incidence has steadily increased in many countries over the past several decades [1, 2]. Papillary thyroid carcinoma (PTC) is the most

\*Correspondence: haozhang@cmu.edu.cn

<sup>1</sup> Department of Thyroid Surgery, The First Hospital of China Medical University, Shenyang, China

Full list of author information is available at the end of the article



© The Author(s) 2021. **Open Access** This article is licensed under a Creative Commons Attribution 4.0 International License, which permits use, sharing, adaptation, distribution and reproduction in any medium or format, as long as you give appropriate credit to the original author(s) and the source, provide a link to the Creative Commons licence, and indicate if changes were made. The images or other third party material in this article are included in the article's Creative Commons licence, unless indicated otherwise in a credit line to the material. If material is not included in the article's Creative Commons licence and your intended use is not permitted by statutory regulation or exceeds the permitted use, you will need to obtain permission directly from the copyright holder. To view a copy of this licence, visit <http://creativecommons.org/licenses/by/4.0/>. The Creative Commons Public Domain Dedication waiver (<http://creativecommons.org/publicdomain/zero/1.0/>) applies to the data made available in this article, unless otherwise stated in a credit line to the data.

universal type of TC, accounting for more than 80% of all cases, with a high 10-year survival rate over 90% [3, 4]. Although the majority of PTC remain indolent, tumor recurrence and metastasis obstruct the clinical management and survival in certain patients [5].

Ferroptosis describes a novel form of regulated cell death that occurs as a consequence of lethal lipid peroxidation, which is distinct from the apoptosis, necroptosis and pyroptosis [6, 7]. It can be induced by experimental compounds or clinical drugs, such as erastin, ras-selective lethal small molecule 3 (RSL3), or sorafenib, in cancer cells and certain normal cells [8]. It's worth noting that sorafenib was approved by the Food and Drug Administration (FDA) for the treatment of multiple types of advanced cancer, including TC [9–12]. Ferroptosis has been implicated in the pathological cell death and its dysregulation has been associated with carcinogenesis, such as pancreatic cancer, hepatocellular carcinoma, kidney and ovary. Ferroptosis may also have a tumor suppressor function that could be harnessed for cancer therapy [13–16]. In addition, a line of evidence from several researches demonstrate the ferroptotic cells could interact with immune cells, such as CD8+ T cells, by releasing chemotaxis, and then modulating the anticancer immunity [17–21]. Lately, ferroptosis was found to be induced in anaplastic thyroid cancer (ATC) by vitamin C via the inactivation of GPX4, reactive oxygen species (ROS) accumulation and iron sustained lipid peroxidation [22]. Numerous studies have reported that ferroptosis-related genes (FRGs) play a pivotal role in predicting tumor prognosis [23–25], however, the association between FRGs and prognosis in patients with PTC remains to be elucidated.

This study aims at exploring the expression of FRGs and their prognostic value in PTC. Differential expression of FRGs was used to establish a prognostic multi-gene signature. Additionally, we explored the underlying mechanism of the FRGs signature by a series of analyses to illustrate its prognostic value. Finally, signature genes were tested in clinical PTC specimens and adjacent normal thyroid tissues.

## Materials and methods

### Acquisition of gene expression and clinical data

The mRNA sequencing (RNA-seq) data and corresponding clinical information of 507 PTC patients were downloaded from the TCGA database (<https://portal.gdc.cancer.gov/repository>). The dataset included 510 PTC tissue samples and 58 adjacent normal tissue samples. The gene expression profiles were normalized using the Perl language (<http://www.perl.org/>). The corresponding FRGs were downloaded from FerrDb (<http://www.zhounan.org/ferrdb/index.html>), a web-based consortium that

provided a comprehensive and up-to-date database for ferroptosis markers, regulatory molecules and associated diseases [26]. After eliminating duplicate items from the whole genes (driver: 150; suppressor: 109; marker: 123), we identified 259 FRGs (Additional file 1). The clinical information for 507 patients was presented on Table 1.

### Prognostic validity of the gene signature

Differentially expressed genes (DEGs) related to ferroptosis in tumor tissues and adjacent normal tissues in the TCGA PTC cohort were described using the 'limma' package in R (version 4.0.4; <https://www.r-project.org/>), with a false-discovery rate (FDR) < 0.05. FRGs related to overall survival (OS) were identified with univariate Cox regression analysis. Ferroptosis-related DEGs were used to construct a protein–protein interaction network with a minimum required interaction score  $\geq 0.15$

**Table 1** Demographic and clinical characteristics of patients in the Cancer Genome Atlas papillary thyroid cancer cohort and validated papillary thyroid cancer cohort

Clinicopathological features	TCGA(N=507)	Validated Cohort(N=75)
Age (year)		
Mean (SD)	47.26 (15.78)	44.09 (12.65)
< 55岁	340 (67.06%)	57 (76.00%)
$\geq 55$ 岁	167 (32.94%)	18 (24.00%)
Gender, n (%)		
Male	136 (26.82%)	19 (25.33%)
Female	371 (73.18%)	56 (74.67%)
Stage, n (%)		
Stage I	285 (56.21%)	61 (81.33%)
Stage II	52 (10.26%)	8 (10.67%)
Stage III	114 (22.49%)	4 (5.33%)
Stage IV	55 (10.85%)	2 (2.67%)
Unknown	2 (0.39%)	0 (0.00%)
T status, n (%)		
T1	144 (28.40%)	46 (61.33%)
T2	167 (32.94%)	5 (6.67%)
T3	171 (33.73%)	14 (18.67%)
T4	23 (4.54%)	10 (13.33%)
TX	2 (0.39%)	0 (0.00%)
N status, n (%)		
N0	231 (45.56%)	25 (33.33%)
N1	226 (44.58%)	50 (66.67%)
NX	50 (9.86%)	0 (0.00%)
M status, n (%)		
MO	283 (55.82%)	73 (97.33%)
M1	9 (1.78%)	2 (2.67%)
MX	215 (42.41%)	0 (0.00%)

in the STRING database (version 11.0; <https://string-db.org/>). Then, we also explored their correlations using the 'igraph' package in R. The least absolute shrinkage and selection operator (LASSO) Cox regression model was utilized to construct a multigene signature of the ferroptosis-related DEGs in the TCGA cohort by the 'glmnet' package in R. The formula was established as follows: score = e sum (each gene's expression  $\times$  corresponding coefficient). The patients were stratified into high-risk and low-risk groups based on the median value of the risk score. The OS and disease-free survival (DFS) differences between high-risk and low-risk groups were compared by the 'survival' and 'survminer' package in R. Kaplan–Meier curve was implemented to visualize the survival. The receiver operating characteristic (ROC) analysis was used to examine the sensitivity and specificity of survival prediction using the independent risk factors by the 'timeROC' package in R. Univariate and multivariate Cox regression analyses were performed to determine the prognostic value of the risk score and various clinical characteristics. Hazard ratios (HRs) and 95% confidence intervals (CIs) were estimated. For the clinical stratified analysis, patients were divided into different subgroups according to the clinicopathologic features, include age, gender, stage and TNM stages. Kaplan–Meier survival analysis was presented by the 'survival' and 'survminer' package in R between high and low risk score groups in different subgroups.

#### Functional enrichment analysis

The "clusterProfiler" R package was utilized to conduct Gene Ontology (GO) and Kyoto Encyclopedia of Genes and Genomes (KEGG) analyses based on the DEGs ( $|\log_2FC| \geq 1$ , FDR < 0.05) between the high-risk and low-risk groups.

#### Immune-related analysis

Immune infiltration in PTC was investigated by calculating single-sample gene set enrichment analysis (ssGSEA) scores of 16 immune cells and 13 immune-related pathways using the 'gsva' package in R. The correlation between the prognostic signature and immune cells was performed by Pearson correlation analysis via CIBERSORT (<http://cibersort.stanford.edu/>).

#### Statistical analysis

Data were all analyzed using Bioconductor packages in R software. The significance of the differences in the expression of FRGs between tumor and normal tissues was assessed by the Wilcoxon test. Univariate and multivariate cox regression analyses were used to evaluate the correlation between the affecting factors and patients' OS or DFS. Mann–Whitney test with *P* values adjusted

by the Benjamini-Hochberg (BH) method was used to compare the ssGSEA scores of immune cells or pathways between the high-risk and low-risk groups. *P* value < 0.05 was set as statistically significant for all the analyses.

#### Quantitative real-time PCR

Quantitative Real-Time PCR (qRT-PCR) was performed on 75 pairs of tumor tissues and adjacent normal tissues to validate the mRNA expression levels of the ten signature genes. Consent form was obtained from each patient involved in this study, and the study approved by the Ethics Committee of the First Hospital of China Medical University (Ethical Approval Number: [2021]82). The clinical information for the 75 patients was presented on Table 1. Total RNA was extracted from the sample tissues via RNAiso Plus (TAKARA, China), followed by reverse transcription into cDNA. qRT-PCR was carried out using the TB Green R Premix Ex Taq™ II kit (TAKARA, China). GAPDH served as an internal control. The relative expression levels were quantified by the Ct ( $2^{-\Delta\Delta Ct}$ ) method. The primer sequences were listed (Table 2).

#### Cell culture and reagents

Human thyroid cancer cell lines K1 (European Collection of Cell Cultures) and KTC-1 (Chinese Academy of Sciences Stem Cell Bank) were cultured in RPMI-1640,

**Table 2** Primer sequences for qRT-PCR

Primer	Sequence (5'-3')
ANGPTL7-F	TAGAGATGGAGGACTGGGAGG
ANGPTL7-R	GTGCACACTTGTCCAAGCAG
CDKN2A-F	GGGAGCAGCATGGAGCCG
CDKN2A-R	CTGGATCGGCCTCCGACCCTA
DPP4-F	AGTGGCGTGTCAAGTGT
DPP4-R	AGTGGCTCATGTGGGTAT
DRD4-F	GGGAAGGACAGTGTCTGGATCTG
DRD4-R	AGTGCTCTAGATAAGTTGGCAAATGCA
ISCU-F	CCAGTGATGAAAAGGGGAA
ISCU-R	GCAGAGTTCCTTGCGCATGT
Srxn1-F	CCCACTGGACCACTTCTGT
Srxn1-R	GTGGCTAGCTCAGACCAAGG
TXNRD1-F	AAATTCTTAGACGGTCCGGG
TXNRD1-R	AGTCTGCCCTCTGATAAGC
TFRC-F	TCAGTTTCCACCATCTCG
TFRC-R	AAGTCTCCAGCACTCCAA
TF-F	TCAGCAGAGACCACCGAAGACT
TF-R	GACCACACTTGCCCGCTATGTA
PGD-F	GTTCCAAGACACCGATGGCAAAC
PGD-R	CACCGAGCAAAGACAGCTTCTC
GAPDH-F	GTCTCCTCTGACTTCAACAGCG
GAPDH-R	ACCACCCTGTTGCTGTAGCCAA

comprising 10% fetal bovine serum (FBS), 1% non-essential amino acids(NEAA), 1% Glutamax and 1% Sodium Pyruvate at the humidified chamber of 37 °C and 5% CO<sub>2</sub>. on. Sorafenib (S7397) was obtained from Selleck( Houston, TX, USA).

**Cell viability assay**

Cells (3000 to 4000/well) were seeded in 96-well plates. After a 24 h culture, cells were treated with different doses of sorafenib for 24 h. The Cell Counting Kit-8(CCK-8; MedChem Express, China) assay was then carried out to assess the effect of sorafenib on cell viability, and IC<sub>50</sub> values were calculated according to the instructions.

**Transmission electron microscopy (TEM)**

Cell samples were fixed with 2.5% glutaraldehyde, dehydrated in acetone solutions at increasing concentrations, and embedded in an epoxy resin. Then, the

Sections (70–90 nm) were stained with lead citrate and uranyl acetate. Ultrastructural images were then captured with a transmission electron microscope (Hitachi H7650, Japan).

**Results**

**Identification of 15 differentially expressed prognostic FRGs**

Most of the FRGs (176/259, 68.0%) were differentially expressed between tumor and adjacent normal tissue, and 15 of them were correlated with OS in the univariate Cox regression analysis (Fig. 1A, B). The heatmap exhibited the expression difference of 15 intersect genes between tumor tissues and adjacent nontumorous tissues (Fig. 1C). The correlation network and protein–protein interaction network provided interactive information among these differentially expressed prognostic FRGs (Fig. 1D, E).

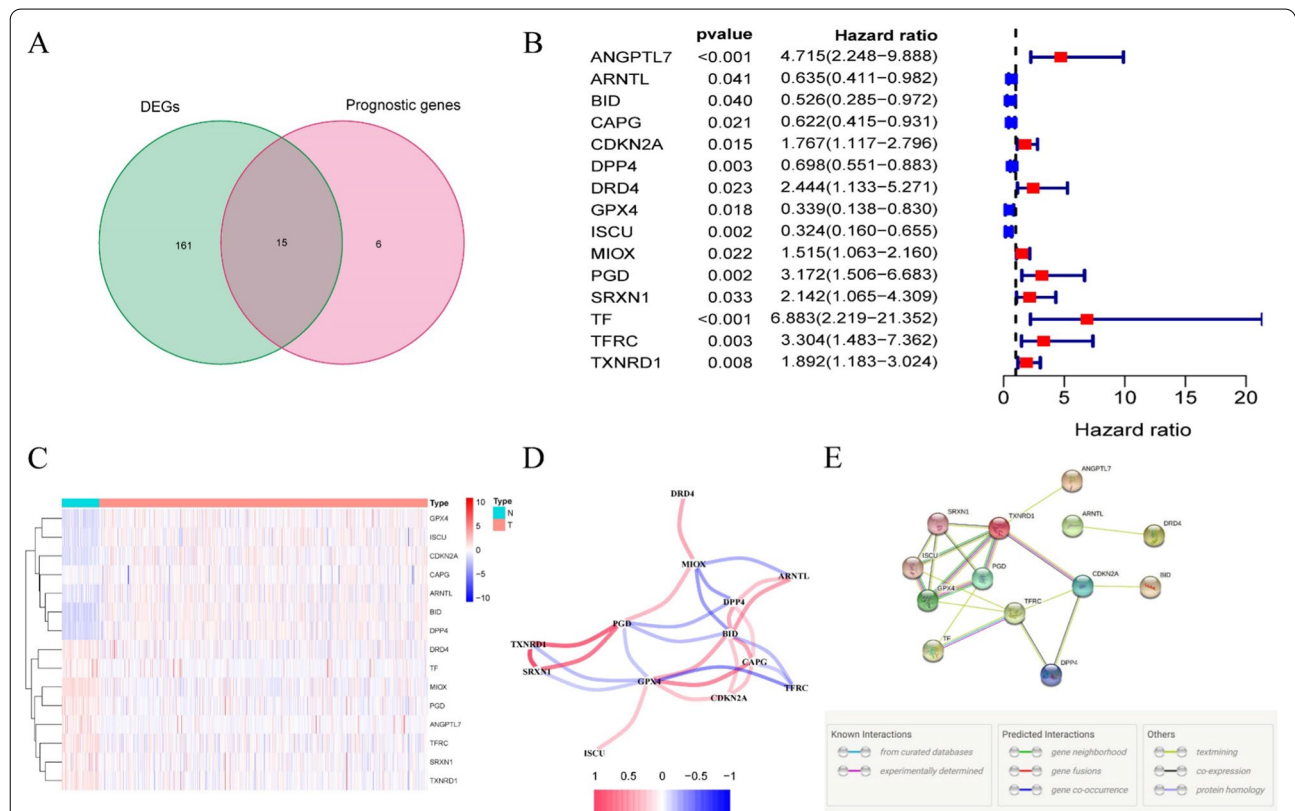


**Fig. 1** Identification of differentially expressed genes related to ferroptosis in TCGA papillary thyroid cancer cohort. **A** 15 out of 21 prognostic ferroptosis-related genes were differentially expressed between tumor tissues and adjacent normal tissues; **B** univariate Cox proportional regression analysis showed the 15 differentially expressed prognostic ferroptosis-related genes were significantly associated with overall survival; **C** the heatmap of the expression of 15 differentially expressed prognostic ferroptosis-related genes in tumor and normal thyroid. **D** the correlation network of 15 differentially expressed prognostic ferroptosis-related genes. Correlation coefficients are represented by different colors. **E** the PPI network provided interactive information among the 15 differentially expressed prognostic ferroptosis-related genes

### Establishment of a 10-FRGs signature predicting the prognosis of PTC

Lasso Cox regression analysis was utilized based on the 15 differentially expressed prognostic FRGs, and a 10-gene signature was constructed. The risk score for each patient was calculated using the following formula: risk score = ANGPTL7 × 1.52040 + CDKN2A × 0.28426 + DPP4 × (- 0.15329) + DRD4 × 0.56101 + ISCU × (- 0.55270) + PGD × 0.31588 + SRXN1 × 0.29977 + TF × 1.38073 + TFRC × 0.60187 + TXNRD1 × 0.15114. Patients were classified as high risk (n = 250) or low risk (n = 251) based on their signature-based risk scores (Fig. 2A, the median value of the risk score = 0.691487). The scatter diagram showed the patients survival status (Fig. 2B). Kaplan–Meier survival curves confirmed that OS and DFS were significantly worse in high-risk compared with low-risk patients (Fig. 2C, D). When the risk score > 1.72, the patient’s mean 5-year survival is < 50% (Additional file 2). Time-dependent ROC curves were used to evaluate the predictive performance of the signature-based

risk score for OS. The area under the curve values were: 0.949 for 1-year OS, 0.900 for 3-year OS, and 0.859 for 5-year OS, respectively (Fig. 2E). The heatmap indicated the significant differences in gender and N stage between high- and low-risk groups (Fig. 2F).

### The 10-genes signature is an independent prognostic indicator for OS and DFS

Univariate and multivariate Cox regression analyses were carried out among the available variables to come to the conclusion that the risk score was an independent prognostic predictor for OS (Fig. 3A, B; univariate: HR = 4.753, 95% CI = 3.053–7.400, P < 0.001; multivariate: HR = 3.680, 95% CI = 2.380–5.691, P < 0.001). Univariate and multivariate Cox regression analyses were carried out to the conclusion that the risk score was significantly associated with DFS (Fig. 3c, D; univariate: HR = 5.946, 95% CI = 1.910–18.514, P < 0.01; multivariate: HR = 4.957, 95% CI = 1.339–18.359, P < 0.05).

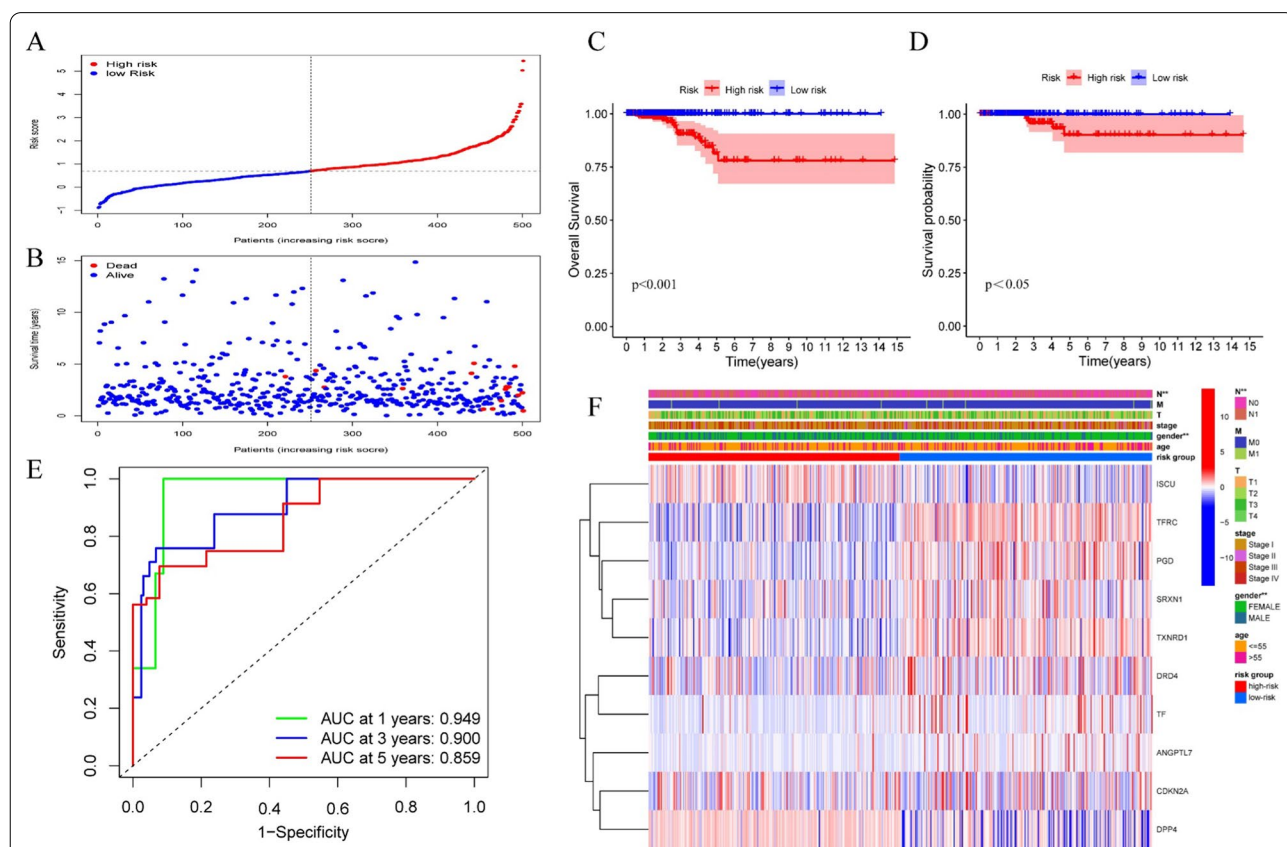
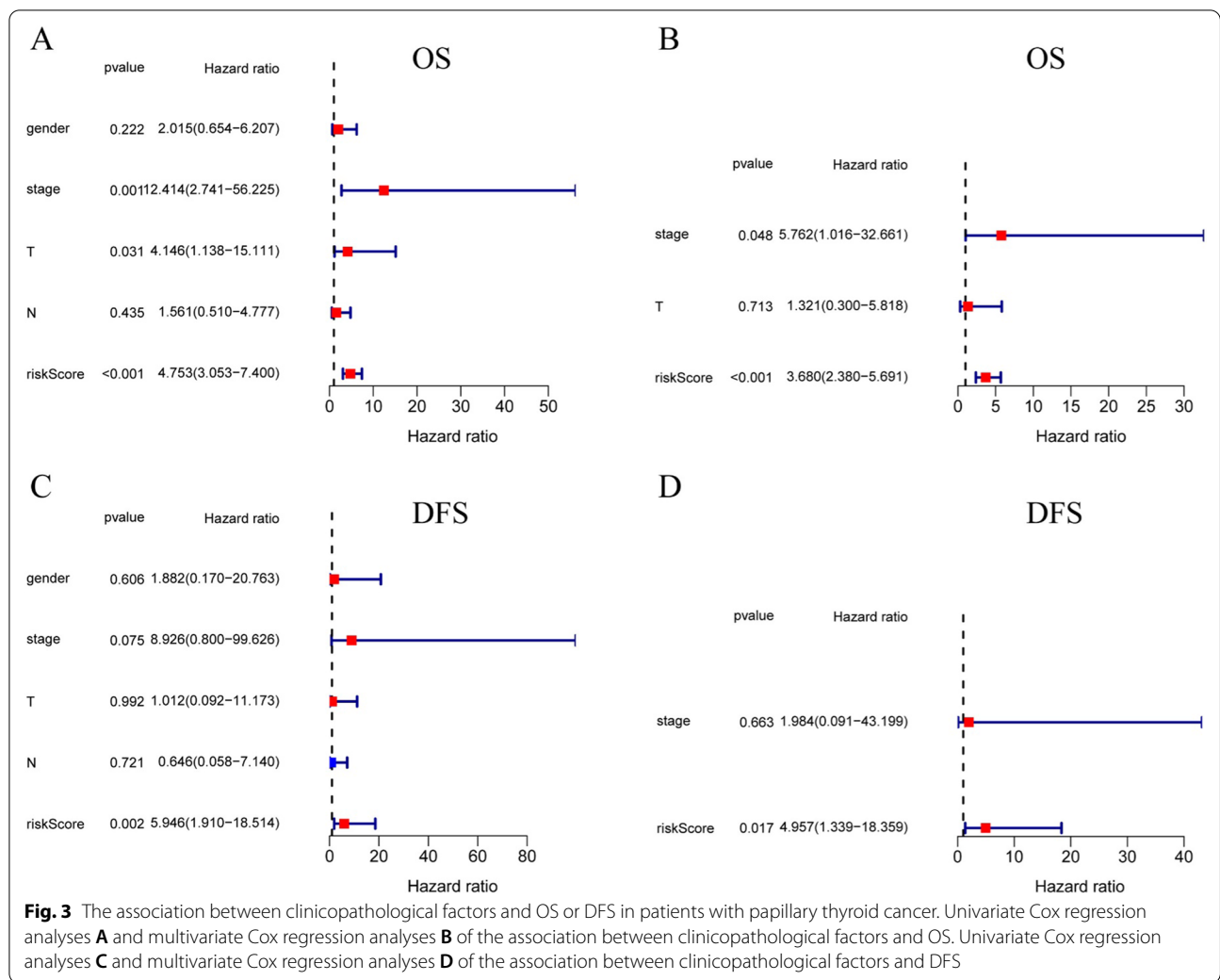


**Fig. 2** Establishment of a ferroptosis-related gene signature in TCGA papillary thyroid cancer cohort. **A** Signature-based risk scores were used to classify patients as high risk or low risk; **B** survival of high-risk and low-risk patients; **C** Kaplan–Meier curves for overall survival (P < 0.001); **D** Kaplan–Meier curves for disease free survival (P < 0.05); **E** time-dependent receiver operating characteristic curves validated the predictive performance of the signature-based risk score for overall survival; **F** the heatmap for ferroptosis-related genes prognostic signature and clinicopathological manifestations (\*P < 0.05, \*\*P < 0.01, \*\*\*P < 0.001)



**Clinical stratified analysis verifies the signature’s forecasting performance**

Clinical stratified analysis was performed to evaluate the forecasting performance of the ten- gene signature (Fig. 4). Although there were no significant difference between high and low risk groups in the OS of three groups (patients with age ≤ 55, N0 and M1), the other 9 clinical groups demonstrated that the high-risk score signified a poorer prognosis in comparison to low-risk score.

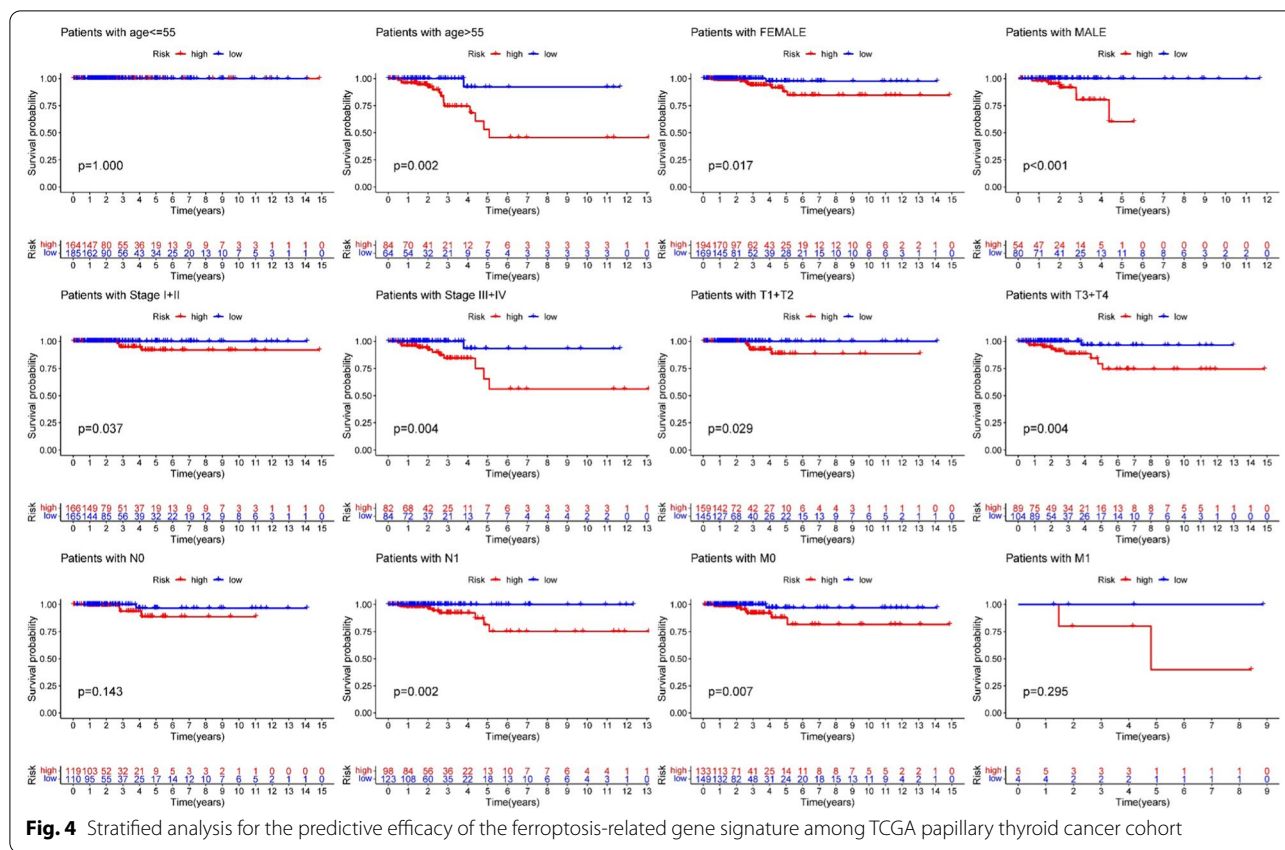
**GO and KEGG analyses**

The functional roles of the DEGs in high- and low-risk patients in the TGCA cohort were explored using GO enrichment and KEGG pathway analyses. GO analysis showed that the DEGs were mostly enriched in several hormone metabolic processes, especially the thyroid hormone (Fig. 5A, B). Beyond that, enrichment was also observed in the metabolism of lipid and the activation

of receptor (*q* value < 0.05). KEGG analysis showed that DEGs were mostly enriched in the thyroid hormone synthesis and immune-related pathways such as the PPAR signaling pathway (Fig. 5C, D; *q* value < 0.05).

**Immune function analysis found that the signature is closely related to the immune cells**

To further explore the correlation between the risk score and immune status, we quantified the enrichment scores of diverse immune cell subpopulations, related functions or pathways with ssGSEA. The results showed the accumulation of various immune cells (such as aDCs, B cells, DCs, iDCs, mast cells, NK cells, Tfh cells and Treg cells) with tumor microenvironment (TME) in the high-risk group were significantly different with those in the low-risk group (Fig. 6A). Moreover, the scores of the immune functions, such as the APC co-stimulation, HLA, MHC class I and Type I IFN response were significantly higher in low-risk group, which indicated anti-tumor



immunological function was more active in the low-risk group (Fig. 6B).

The CIBERSORT database was used to better understand characteristics of immune cells and FRGs signature (Fig. 6C). The risk score of the 10-gene signature has negative correlations with aDCs ( $P < 0.01$ ), APC co-stimulation ( $P < 0.05$ ), DCs ( $P < 0.05$ ), HLA ( $P < 0.01$ ), iDCs ( $P < 0.01$ ), mast cells ( $P < 0.001$ ), MHC class I ( $P < 0.01$ ) and NK cells ( $P < 0.001$ ), while positive correlations with B cell ( $P < 0.001$ ) and Tfh ( $P < 0.001$ ).

**Verification of the 10 included genes by clinical specimens and cell experiments**

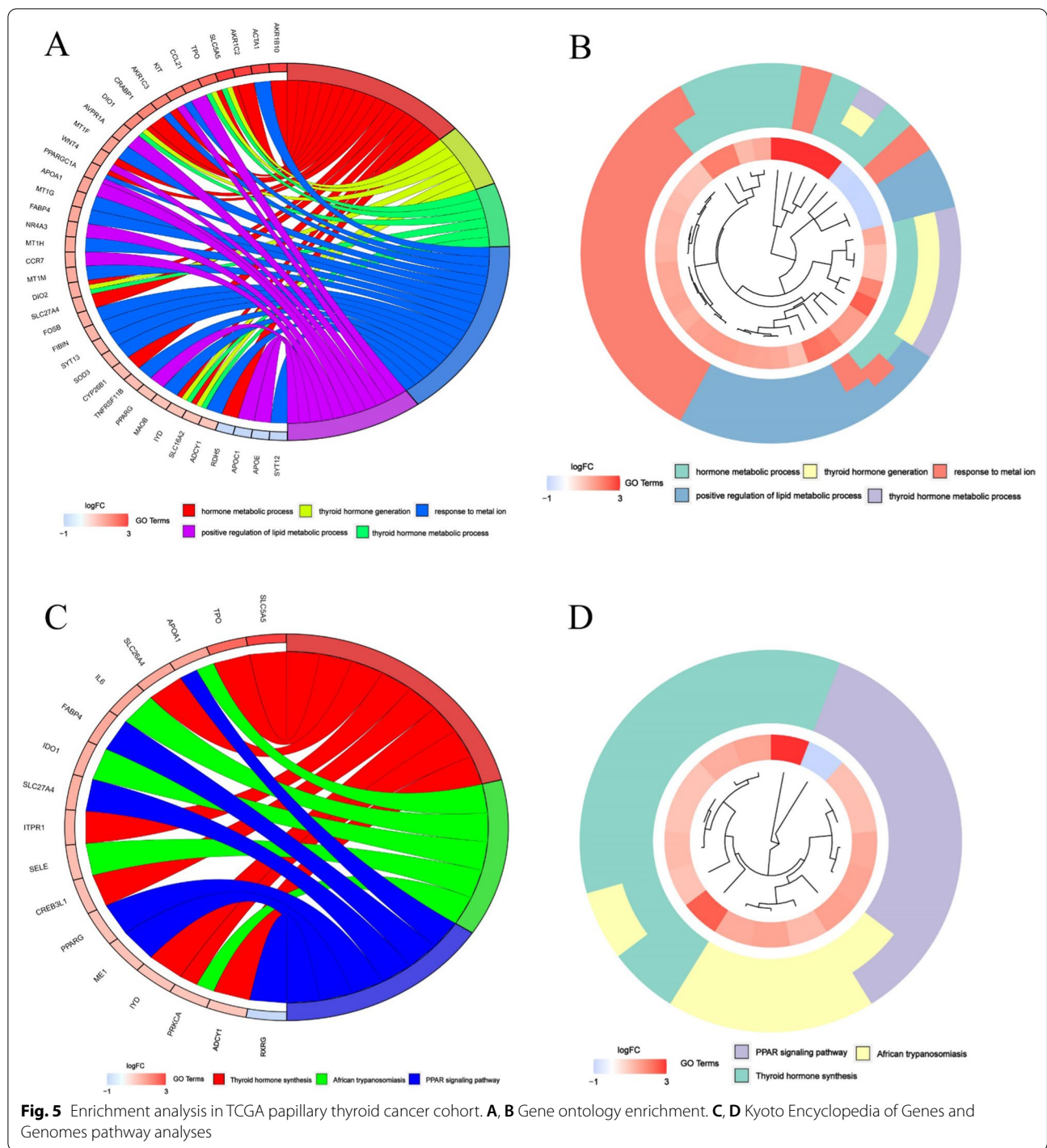
The qRT-PCR was performed on 75 pairs of tumor tissues and adjacent normal tissues to validate the mRNA expression levels of the ten signature genes. The PCR results showed ISCU and TXNRD1 were down-regulated, while the most genes were significantly up-regulated in the PTC tissues. There were no significant differences in the expression of TFRC between the normal and PTC specimens (Fig. 7. \* $P < 0.05$ ; \*\* $P < 0.01$ , \*\*\* $P < 0.001$ , ns: not significant). All results were mainly consistent with the data in TCGA.

Sorafenib were used in further experiments of thyroid cancer cell lines, as a common inducer of ferroptosis

and approved drug for thyroid cancer. TEM showed the ultrastructure of the KTC-1 cell line in control group and 10  $\mu$ M sorafenib for 24 h. White arrowheads indicate ruptured membrane and the shrunken inner cristae of mitochondria (Fig. 8A, B). K1 and KTC-1 cells were treated with different doses of sorafenib for 24 h, and cell viability was measured by Cell Counting Kit-8. It was found that K1 is more sensitive to sorafenib than KTC-1 (Fig. 8C,  $p < 0.01$ ). And we found that the risk score of KTC-1 was higher than K1 (Fig. 8D). The PCR results showed the expression of most genes were significantly changed under the influence of sorafenib. (Fig. 8E, \* $P < 0.05$ , \*\* $P < 0.01$ , \*\*\* $P < 0.001$ , ns: not significant).

**Discussion**

Thyroid cancer is the most common endocrine malignancy with a rapidly increasing incidence worldwide [27]. Although the majority of PTC patients have an excellent prognosis, there are also some patients with recurrence, distant metastasis and even other worse ending, affecting the survival time of patients [28, 29]. Therefore, it is particularly important to carry out risk stratification management to optimize the therapy for PTC patients. Ferroptosis has been proved to participate in tumor proliferation and metastasis, and is closely related to TME

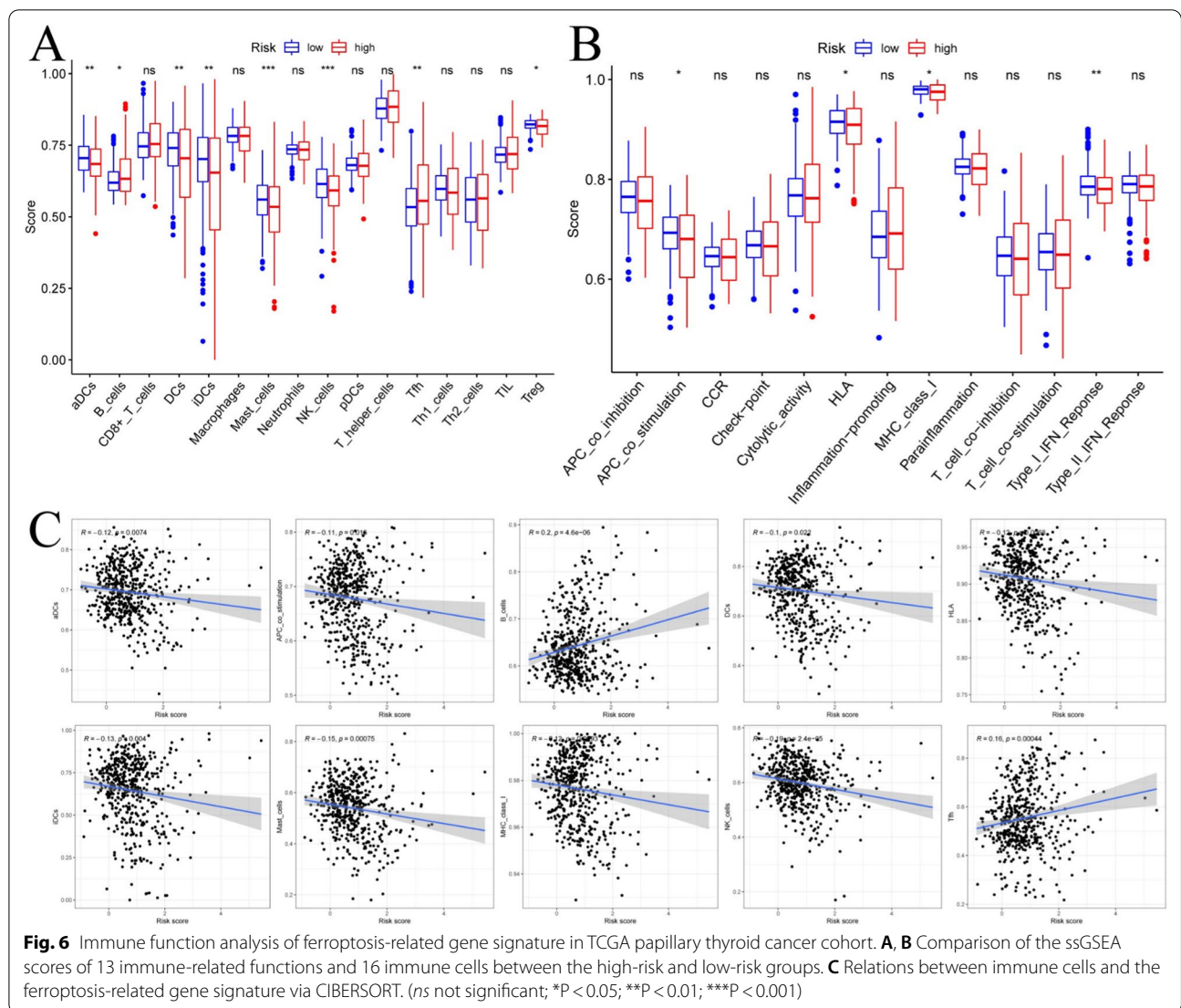


and tumor immunity [30, 31]. In this study, we developed a FRGs signature to predict the prognosis of PTC.

From the 15 differentially expressed prognostic FRGs, we established a 10-gene signature. The high expression of ANGPTL7, CDKN2A, DRD4, PGD, SRXN1, TE, TFRC, TXNRD1 represent high risk score and worse

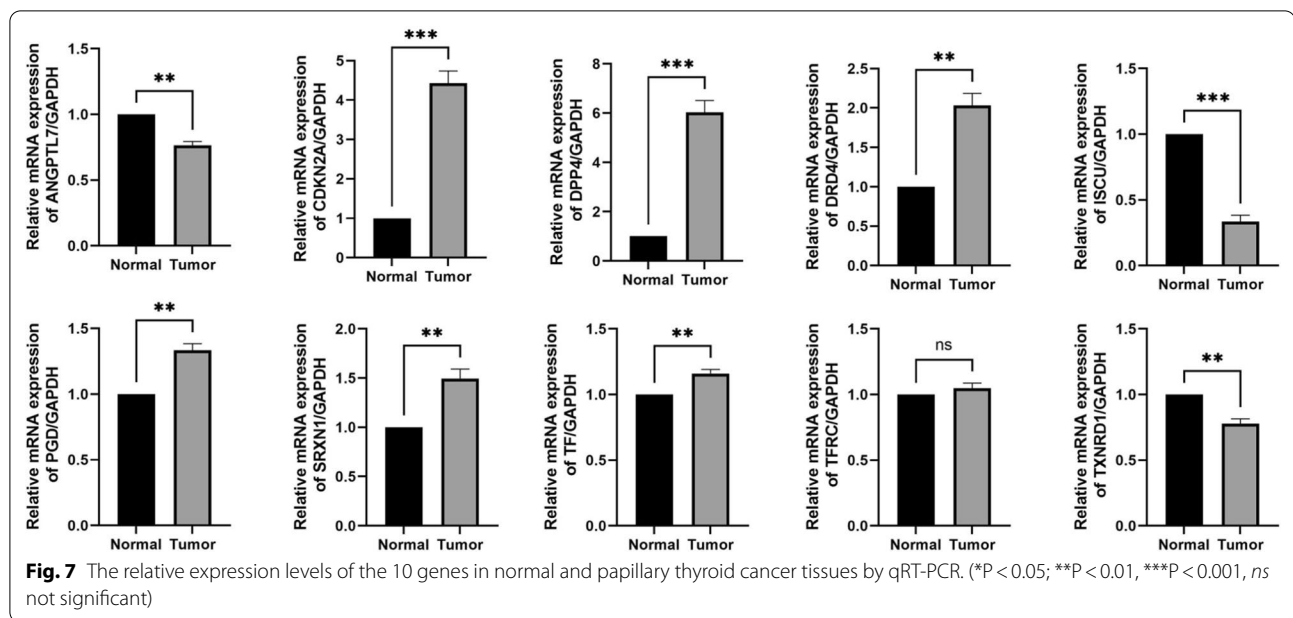
prognosis, conversely, the high expression of DPP4 and ISCU were associated with lower risk in PTC. ANGPTL7 is the less characterized member of the Angiopoietin-like (ANGPTL) proteins families, who can stimulate human differentiated endothelial cell's proliferation, motility and invasiveness [32]. Existing research findings implicated





ANGPTL7 was a mediator of metastatic progression and a potential target for interference with cancer metastases [33]. Although CDKN2A/p16 is a known tumor suppressor gene, CDKN2A hypermethylation might be a predictive factor for unfavorable prognosis of portion cancer [34]. According to research findings, high level of DRD4 expression has worse survival than low of DRD4 expression in Glioblastomas [35]. DRD4 might regulate chemosensitivity of cancer via inhibiting ferroptosis [36]. Decreasing PGD phosphorylation through EGFR signaling could dramatically attenuate cancer cells' proliferation, growth and resistance to ionizing radiation [37]. Beyond that PGD inhibition significantly inhibits growth and survival of ATC cells and sensitizes ATC cells to doxorubicin treatment [38]. SRXN1 is a pivotal regulator of the antioxidant response in eukaryotic cells. SRXN1 could promotes tumor growth and metastasis

and correlates with worse prognosis and decreased survival in different carcinoma [39, 40]. TF and TFRC are two key molecules in transportation of iron ion during ferroptosis, and both genes were low expressed in tumor tissues. TF could co-work with thyroid hormones in differentiation and other biological processes, and serum TF may also have a further role in stimulating cell proliferation [41, 42]. TFRC is a specific ferroptosis marker and may could characterize the extent of ferroptosis [43]. The silencing of TFRC gene reduces liver cancer cell growth and survival [44]. Regulation of TXNRD1 could affect the proliferation, invasion and migration of carcinoma [45, 46]. The inhibition of TrxR1 blocks STAT3 activity and induces cancer cell death [47]. DPP4 has been reported as prognostic marker and therapeutic target of PTC [48]. The activity of DPP4 could down-regulation by TP53 to limits erastin-induced ferroptosis [49]. ISCU, a

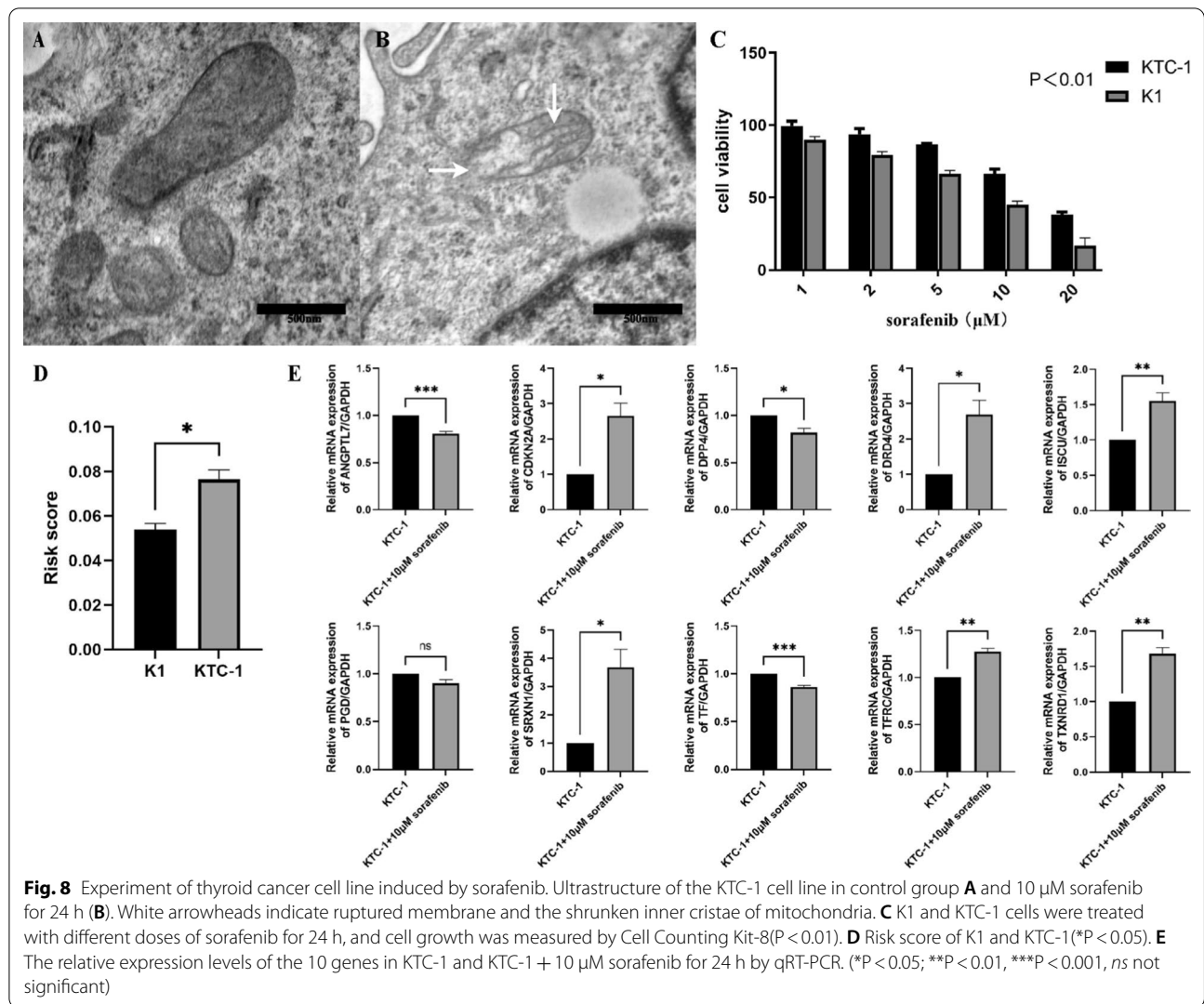


mitochondrial protein, significantly attenuates ferroptosis by regulating iron metabolism, rescuing the mitochondrial function and increasing the level of GSH [50]. Influenced by TP53, the expression of ISCU is related with the maintenance of iron homeostasis in hepatocellular carcinogenesis [51]. It should be noted that the relationship of ten signature's genes with ferroptosis and thyroid cancer requires further clarification.

Functional analyses showed that the DEGs in the high-risk and low-risk patients identified in the present study were enriched in PPAR signaling pathway, which is existed as three different isoforms ( $\alpha$ ,  $\gamma$ , and  $\delta$ ) that play major roles in adipose tissue development and lipid metabolism [52, 53]. PPARs are expressed in immune cells and have an emerging critical role in immune cell differentiation and fate commitment [54]. Moreover, previous studies founded that PPAR $\alpha$  activity is essential to regulate lipids through promoting ferroptosis [55]. Presented data suggested that PPAR $\gamma$  may promote growth and invasion of cancer cells and play a detrimental role in thyroid cancer [56, 57]. The metabolic processes of thyroid hormone (TH) have a certain influence on the proliferation and anti-apoptosis of thyroid cancer [58]. The existed research shows that the TH effects the differentiation and microenvironment of various tumors [59, 60]. Targeting TH in the thyroid cancer may improve treatment strategies.

There is a tight crosstalk between ferroptosis and antitumor immunity [61]. Different immune cells and mediators can contribute to thyroid cancer development and progression through various functional pathways [62, 63]. This study found that several kinds

of tumor-specific cellular immunity and immune-related functions were altered in high-risk compared with low-risk patients. The previous study found that the accumulation of DCs in PTC was possibly correlated with favorable clinical course [64]. iDC were markedly reduced in poorly differentiated thyroid carcinoma (PDTTC) and anaplastic thyroid carcinoma (ATC) [65], which partly supported the differences in iDCs between the high and low risk groups in the signature. The increasing of NK cells in the tumor microenvironment has an inversely correlate with advanced stages in patients with PTC [66]. The suppression of NK cell cytotoxicity and differentiation contributed to immune escape of thyroid cancer [67]. Ferritin heavy chain in tumor cells may modulate the expression of MHC class I molecules and influence NK cells, which may explain the association between ferroptosis and NK activation [68]. It has been reported that the exacerbation of ferroptosis via activating IFN- $\gamma$ /ASK1/JNK signaling pathway [69] revealed the possible connection between the IFN- $\gamma$  and ferroptosis. Type II IFN response played a pivotal function on cancer immune surveillance, stimulating antitumor immunity and promoting tumor recognition and elimination [70]. The prognostic signature showed a statistically significant negative correlation with most immune cells, at the same time, the immune score of the high-risk group is just below the low-risk group. Previous research demonstrated that mast cells have a contributing to thyroid carcinoma growth and invasiveness [71]. It was reported that mast cells infiltration was correlated with extrathyroidal extension of tumors



and tumor invasiveness [72]. But the low numbers of tryptase mast cells were also associated with poor OS and more advanced stage [73]. The role of mast cells in PTC prognosis warrants further research.

The number of bioinformatics articles about ferroptosis is huge, and there are some similarities inevitably. In our manuscript, the signature was not only related to OS, but also related to DFS of thyroid cancer. So, the signature has better predictive performance. In addition, we stimulated thyroid cancer cell by sorafenib, and verified the expression change of the signature genes.

Although we verified the ten signature genes expression in 75 pairs of tumor tissues and paracancerous tissues, as well as PTC cell lines induced by sorafenib, by qRT-PCR and got a result that almost matched the TCGA, the prognostic predictive value of the ten-gene signature is based on a single cohort. Future studies

involving larger independent cohorts should be conducted to validate our findings.

### Conclusion

In conclusion, here we revealed the expression and prognostic value of FRGs in PTC. Additionally, we developed a risk signature that divided PTC patients into high-risk and low-risk groups with significantly different OS and DFS. These results may allow clinicians to determine individualized treatment for PTC patients with different clinical features and provide crucial evidence supporting further research of the role of ferroptosis in PTC.

### Supplementary Information

The online version contains supplementary material available at <https://doi.org/10.1186/s12935-021-02389-7>.

**Additional file 1.** A list of 259 ferroptosis-related genes identified from FerrDb.

**Additional file 2.** Kaplan–Meier curves for overall survival at the best cut-off value of the risk score.

### Acknowledgements

Not applicable.

### Authors' contributions

JY SHI performed the data analysis and wrote the manuscript. WP helped to accurately process the data. SL, SW and ZH reviewed and revised the manuscript. All authors read and approved the final manuscript.

### Funding

This work was supported by the National Natural Science Foundation of China (81902726), China Postdoctoral Science Foundation (2018M641739), Shenyang Science and Technology Bureau (213408), Shenyang Department of Education (QNZR2020002).

### Availability of data and materials

Gene expression profiles, clinical information and mutation data of THCA in this study are available from the public database (TCGA, <https://portal.gdc.cancer.gov/>).

### Declarations

#### Ethics approval and consent to participate

The study was approved by the Ethics Committee of the First Hospital of China Medical University (Shenyang, China).

#### Consent for publication

Not applicable.

#### Competing interests

The authors declare that the research was conducted in the absence of any commercial or financial relationships that could be construed as a potential conflict of interest.

#### Author details

<sup>1</sup>Department of Thyroid Surgery, The First Hospital of China Medical University, Shenyang, China. <sup>2</sup>Department of Thyroid Surgery, General Surgery, Qilu Hospital of Shandong University, Jinan, Shandong, China.

Received: 2 September 2021 Accepted: 3 December 2021

Published online: 14 December 2021

### References

- James BC, Mitchell JM, Jeon HD, Vasilottos N, Grogan RH, Aschebrook-Kilfoy B. An update in international trends in incidence rates of thyroid cancer, 1973–2007. *Cancer Causes Control*. 2018;29(4–5):465–73.
- Pellegriti G, Frasca F, Regalbuto C, Squatrito S, Vigneri R. Worldwide increasing incidence of thyroid cancer: update on epidemiology and risk factors. *J Cancer Epidemiol*. 2013;2013:965212.
- Kitahara CM, Sosa JA. The changing incidence of thyroid cancer. *Nat Rev Endocrinol*. 2016;12(11):646–53.
- Ito Y, Miyauchi A, Kihara M, Fukushima M, Higashiyama T, Miya A. Overall survival of papillary thyroid carcinoma patients: a single-institution long-term follow-up of 5897 patients. *World J Surg*. 2018;42(3):615–22.
- Ren H, Shen Y, Hu D, He W, Zhou J, Cao Y, Mao Y, Dou Y, Xiong W, Xiao Q, et al. Co-existence of BRAF(V600E) and TERT promoter mutations in papillary thyroid carcinoma is associated with tumor aggressiveness, but not with lymph node metastasis. *Cancer Manag Res*. 2018;10:1005–13.
- Stockwell BR, Friedmann Angeli JP, Bayir H, Bush AI, Conrad M, Dixon SJ, Fulda S, Gascon S, Hatzios SK, Kagan VE, et al. Ferroptosis: a regulated cell death nexus linking metabolism, redox biology, and disease. *Cell*. 2017;171(2):273–85.
- Dixon SJ, Lemberg KM, Lamprecht MR, Skouta R, Zaitsev EM, Gleason CE, Patel DN, Bauer AJ, Cantley AM, Yang WS, et al. Ferroptosis: an iron-dependent form of nonapoptotic cell death. *Cell*. 2012;149(5):1060–72.
- Xie Y, Hou W, Song X, Yu Y, Huang J, Sun X, Kang R, Tang D. Ferroptosis: process and function. *Cell Death Differ*. 2016;23(3):369–79.
- Cabanillas ME, Ryder M, Jimenez C. Targeted therapy for advanced thyroid cancer: kinase inhibitors and beyond. *Endocr Rev*. 2019;40(6):1573–604.
- Llovet JM, Montal R, Sia D, Finn RS. Molecular therapies and precision medicine for hepatocellular carcinoma. *Nat Rev Clin Oncol*. 2018;15(10):599–616.
- Escudier B, Eisen T, Stadler WM, Szczylik C, Oudard S, Siebels M, Negrier S, Chevreau C, Solska E, Desai AA, et al. Sorafenib in advanced clear-cell renal-cell carcinoma. *N Engl J Med*. 2007;356(2):125–34.
- Abdelgalil AA, Alkahtani HM, Al-Jenoobi FI. Sorafenib. *Profiles Drug Subst Excip Relat Methodol*. 2019;44:239–66.
- Liu J, Dai E, Kang R, Kroemer G, Tang D. The dark side of ferroptosis in pancreatic cancer. *Oncoimmunology*. 2021;10(11):1868691.
- Nie J, Lin B, Zhou M, Wu L, Zheng T. Role of ferroptosis in hepatocellular carcinoma. *J Cancer Res Clin Oncol*. 2018;144(12):2329–37.
- Zou Y, Palte MJ, Deik AA, Li H, Eaton JK, Wang W, Tseng YY, Deasy R, Kost-Alimova M, Dancik V, et al. A GPX4-dependent cancer cell state underlies the clear-cell morphology and confers sensitivity to ferroptosis. *Nat Commun*. 2019;10(1):1617.
- Chen X, Kang R, Kroemer G, Tang D. Broadening horizons: the role of ferroptosis in cancer. *Nat Rev Clin Oncol*. 2021. <https://doi.org/10.1038/s41571-020-00462-0>.
- Wang W, Green M, Choi JE, Gijon M, Kennedy PD, Johnson JK, Liao P, Lang X, Kryczek I, Sell A, et al. CD8(+) T cells regulate tumour ferroptosis during cancer immunotherapy. *Nature*. 2019;569(7755):270–4.
- Sun Y, Chen P, Zhai B, Zhang M, Xiang Y, Fang J, Xu S, Gao Y, Chen X, Sui X, et al. The emerging role of ferroptosis in inflammation. *Biomed Pharmacother*. 2020;127:110108.
- Rothe T, Gruber F, Uderhardt S, Ipseiz N, Rossner S, Oskolkova O, Bluml S, Leitinger N, Bicker W, Bochkov VN, et al. 12/15-Lipoxygenase-mediated enzymatic lipid oxidation regulates DC maturation and function. *J Clin Invest*. 2015;125(5):1944–54.
- Angeli JPF, Krysko DV, Conrad M. Ferroptosis at the crossroads of cancer-acquired drug resistance and immune evasion. *Nat Rev Cancer*. 2019;19(7):405–14.
- Kloditz K, Fadeel B. Three cell deaths and a funeral: macrophage clearance of cells undergoing distinct modes of cell death. *Cell Death Discov*. 2019;5:65.
- Wang X, Xu S, Zhang L, Cheng X, Yu H, Bao J, Lu R. Vitamin C induces ferroptosis in anaplastic thyroid cancer cells by ferritinophagy activation. *Biochem Biophys Res Commun*. 2021;551:46–53.
- Han F, Li W, Chen T, Yao Y, Li J, Wang D, Wang Z. Ferroptosis-related genes for predicting prognosis of patients with laryngeal squamous cell carcinoma. *Eur Arch Otorhinolaryngol*. 2021. <https://doi.org/10.1007/s00405-021-06789-3>.
- Jiang P, Yang F, Zou C, Bao T, Wu M, Yang D, Bu S. The construction and analysis of a ferroptosis-related gene prognostic signature for pancreatic cancer. *Aging*. 2021. <https://doi.org/10.18632/aging.202801>.
- Zhu L, Yang F, Wang L, Dong L, Huang Z, Wang G, Chen G, Li Q. Identification of the ferroptosis-related gene signature in patients with esophageal adenocarcinoma. *Cancer Cell Int*. 2021;21(1):124.
- Zhou N, Bao J. FerrDb: a manually curated resource for regulators and markers of ferroptosis and ferroptosis-disease associations. *Database (Oxford)*. 2020. <https://doi.org/10.1093/database/baaa021>.
- Wiltshire JJ, Drake TM, Uttley L, Balasubramanian SP. Systematic review of trends in the incidence rates of thyroid cancer. *Thyroid*. 2016;26(11):1541–52.
- Povoa AA, Teixeira E, Bella-Cueto MR, Melo M, Oliveira MJ, Sobrinho-Simoes M, Maciel J, Soares P. Clinicopathological features as prognostic predictors of poor outcome in papillary thyroid carcinoma. *Cancers (Basel)*. 2020;12(11):3186.
- Chen B, Shi Y, Xu Y, Zhang J. The predictive value of coexisting BRAFV600E and TERT promoter mutations on poor outcomes and high tumour aggressiveness in papillary thyroid carcinoma: A systematic review and meta-analysis. *Clin Endocrinol (Oxf)*. 2021;94(5):731–42.

30. Wu J, Minikes AM, Gao M, Bian H, Li Y, Stockwell BR, Chen ZN, Jiang X. Intercellular interaction dictates cancer cell ferroptosis via NF2-YAP signaling. *Nature*. 2019;572(7769):402–6.
31. Friedmann Angeli JP, Krysko DV, Conrad M. Ferroptosis at the crossroads of cancer-acquired drug resistance and immune evasion. *Nat Rev Cancer*. 2019;19(7):405–14.
32. Parri M, Pietrovito L, Grandi A, Campagnoli S, De Camilli E, Bianchini F, Marchio S, Bussolino F, Jin B, Sarmientos P, et al. Angiopoietin-like 7, a novel pro-angiogenic factor over-expressed in cancer. *Angiogenesis*. 2014;17(4):881–96.
33. Lim SY, Gordon-Weeks A, Allen D, Kersemans V, Beech J, Smart S, Muschel RJ. Cd11b(+) myeloid cells support hepatic metastasis through down-regulation of angiopoietin-like 7 in cancer cells. *Hepatology*. 2015;62(2):521–33.
34. Xing X, Cai W, Shi H, Wang Y, Li M, Jiao J, Chen M. The prognostic value of CDKN2A hypermethylation in colorectal cancer: a meta-analysis. *Br J Cancer*. 2013;108(12):2542–8.
35. Dolma S, Selvadurai HJ, Lan X, Lee L, Kushida M, Voisin V, Whetstone H, So M, Aviv T, Park N, et al. Inhibition of dopamine receptor D4 impedes autophagic flux, proliferation, and survival of glioblastoma stem cells. *Cancer Cell*. 2016;29(6):859–73.
36. Wang X, Wang ZB, Luo C, Mao XY, Li X, Yin JY, Zhang W, Zhou HH, Liu ZQ. The Prospective value of dopamine receptors on bio-behavior of tumor. *J Cancer*. 2019;10(7):1622–32.
37. Liu R, Li W, Tao B, Wang X, Yang Z, Zhang Y, Wang C, Liu R, Gao H, Liang J, et al. Tyrosine phosphorylation activates 6-phosphogluconate dehydrogenase and promotes tumor growth and radiation resistance. *Nat Commun*. 2019;10(1):991.
38. Ma L, Cheng Q. Inhibiting 6-phosphogluconate dehydrogenase reverses doxorubicin resistance in anaplastic thyroid cancer via inhibiting NADPH-dependent metabolic reprogramming. *Biochem Biophys Res Commun*. 2018;498(4):912–7.
39. Lv X, Yu H, Zhang Q, Huang Q, Hong X, Yu T, Lan H, Mei C, Zhang W, Luo H, et al. SRXN1 stimulates hepatocellular carcinoma tumorigenesis and metastasis through modulating ROS/p65/BTG2 signalling. *J Cell Mol Med*. 2020;24(18):10714–29.
40. Barquilha CN, Santos NJ, Moncao CCD, Barbosa IC, Lima FO, Justulin LA, Pertega-Gomes N, Felisbino SL. Sulfiredoxin as a potential therapeutic target for advanced and metastatic prostate cancer. *Oxid Med Cell Longev*. 2020. <https://doi.org/10.1155/2020/2148562>.
41. Marziali LN, Correale J, Garcia CI, Pasquini JM. Combined effects of transferrin and thyroid hormone during oligodendrogenesis In vitro. *Glia*. 2016;64(11):1879–91.
42. Kan M, Yamane I. Effects of ferrous iron and transferrin on cell proliferation of human diploid fibroblasts in serum-free culture. *In Vitro*. 1984;20(2):89–94.
43. Feng H, Schorpp K, Jin J, Yozwiak CE, Hoffstrom BG, Decker AM, Rajbhandari P, Stokes ME, Bender HG, Csuka JM, et al. Transferrin receptor is a specific ferroptosis marker. *Cell Rep*. 2020;30(10):3411–3423.e3417.
44. Muhammad JS, Bajbouj K, Shafarin J, Hamad M. Estrogen-induced epigenetic silencing of FTH1 and TFRC genes reduces liver cancer cell growth and survival. *Epigenetics*. 2020;15(12):1302–18.
45. Huang S, Zhu X, Ke Y, Xiao D, Liang C, Chen J, Chang Y. LncRNA FTX inhibition restrains osteosarcoma proliferation and migration via modulating miR-320a/TXNRD1. *Cancer Biol Ther*. 2020;21(4):379–87.
46. Hua S, Quan Y, Zhan M, Liao H, Li Y, Lu L. miR-125b-5p inhibits cell proliferation, migration, and invasion in hepatocellular carcinoma via targeting TXNRD1. *Cancer Cell Int*. 2019;19:203.
47. Busker S, Qian W, Haraldsson M, Espinosa B, Johansson L, Attarha S, Kolosenko I, Liu J, Dagnell M, Grander D, et al. Irreversible TrxR1 inhibitors block STAT3 activity and induce cancer cell death. *Sci Adv*. 2020. <https://doi.org/10.1126/sciadv.aax7945>.
48. Lee JJ, Wang TY, Liu CL, Chien MN, Chen MJ, Hsu YC, Leung CH, Cheng SP. Dipeptidyl peptidase IV as a prognostic marker and therapeutic target in papillary thyroid carcinoma. *J Clin Endocrinol Metab*. 2017;102(8):2930–40.
49. Xie Y, Zhu S, Song X, Sun X, Fan Y, Liu J, Zhong M, Yuan H, Zhang L, Billiar TR, et al. The tumor suppressor p53 limits ferroptosis by blocking DPP4 activity. *Cell Rep*. 2017;20(7):1692–704.
50. Du J, Wang TT, Li YC, Zhou Y, Wang X, Yu XX, Ren XY, An YH, Wu Y, Sun WD, et al. DHA inhibits proliferation and induces ferroptosis of leukemia cells through autophagy dependent degradation of ferritin. *Free Radical Bio Med*. 2019;131:356–69.
51. Funauchi Y, Tanikawa C, Lo PHY, Mori J, Daigo Y, Takano A, Miyagi Y, Okawa A, Nakamura Y, Matsuda K. Regulation of iron homeostasis by the p53-ISCU pathway. *Sci Rep-Uk*. 2015. <https://doi.org/10.1038/srep16497>.
52. Wahli W, Braissant O, Desvergne B. Peroxisome proliferator activated receptors: transcriptional regulators of adipogenesis, lipid metabolism and more. *Chem Biol*. 1995;2(5):261–6.
53. Willson TM, Brown PJ, Sternbach DD, Henke BR. The PPARs: from orphan receptors to drug discovery. *J Med Chem*. 2000;43(4):527–50.
54. Christofides A, Konstantinidou E, Jani C, Boussiotis VA. The role of peroxisome proliferator-activated receptors (PPAR) in immune responses. *Metabolism*. 2021;114:154338.
55. Venkatesh D, O'Brien NA, Zandkarimi F, Tong DR, Stokes ME, Dunn DE, Kengmana ES, Aron AT, Klein AM, Csuka JM, et al. MDM2 and MDMX promote ferroptosis by PPARalpha-mediated lipid remodeling. *Genes Dev*. 2020;34(7–8):526–43.
56. Wood WM, Sharma V, Bauerle KT, Pike LA, Zhou Q, Fretwell DL, Schweppe RE, Haugen BR. PPARgamma promotes growth and invasion of thyroid cancer cells. *PPAR Res*. 2011;2011:171765.
57. Toraih EA, Fawzy MS, Abushouk AI, Shaheen S, Hobani YH, Alruwetei AM. Prognostic value of the miRNA-27a and PPAR/RXRalpha signaling axis in patients with thyroid carcinoma. *Epigenomics*. 2020;12(20):1825–43.
58. Liu YC, Yeh CT, Lin KH. Molecular functions of thyroid hormone signaling in regulation of cancer progression and anti-apoptosis. *Int J Mol Sci*. 2019;20(20):4986.
59. Manka P, Coombes JD, Boosman R, Gauthier K, Papa S, Syn WK. Thyroid hormone in the regulation of hepatocellular carcinoma and its microenvironment. *Cancer Lett*. 2018;419:175–86.
60. Ciciatiello AG, Ambrosio R, Dentice M. Thyroid hormone promotes differentiation of colon cancer stem cells. *Mol Cell Endocrinol*. 2017;459:84–9.
61. Tang R, Xu J, Zhang B, Liu J, Liang C, Hua J, Meng Q, Yu X, Shi S. Ferroptosis, necroptosis, and pyroptosis in anticancer immunity. *J Hematol Oncol*. 2020;13(1):110.
62. Galdiero MR, Varricchi G, Marone G. The immune network in thyroid cancer. *Oncimmunology*. 2016;5(6):e1168556.
63. Ferrarini SM, Fallahi P, Galdiero MR, Ruffilli I, Elia G, Ragusa F, Paparo SR, Patrizio A, Mazzi V, Varricchi G, et al. Immune and inflammatory cells in thyroid cancer microenvironment. *Int J Mol Sci*. 2019;20(18):4413.
64. Batistatou A, Zolota V, Scopa CD. S-100 protein+ dendritic cells and CD34+ dendritic interstitial cells in thyroid lesions. *Endocr Pathol*. 2002;13(2):111–5.
65. Ugolini C, Basolo F, Proietti A, Vitti P, Elisei R, Miccoli P, Toniolo A. Lymphocyte and immature dendritic cell infiltrates in differentiated, poorly differentiated, and undifferentiated thyroid carcinoma. *Thyroid*. 2007;17(5):389–93.
66. Gogali F, Paterakis G, Rassidakis GZ, Liakou CI, Liapi C. CD3(–)CD16(–)CD56(bright) immunoregulatory NK cells are increased in the tumor microenvironment and inversely correlate with advanced stages in patients with papillary thyroid cancer. *Thyroid*. 2013;23(12):1561–8.
67. Park A, Lee Y, Kim MS, Kang YJ, Park YJ, Jung H, Kim TD, Lee HG, Choi I, Yoon SR. Prostaglandin E2 secreted by thyroid cancer cells contributes to immune escape through the suppression of natural killer (NK) cell cytotoxicity and NK cell differentiation. *Front Immunol*. 2018. <https://doi.org/10.3389/fimmu.2018.01859>.
68. Sottile R, Federico G, Garofalo C, Talerico R, Faniello MC, Quaresima B, Cristiani CM, Di Sanzo M, Cuda G, Ventura V, et al. Iron and ferritin modulate MHC class I expression and NK cell recognition. *Front Immunol*. 2019;10:224.
69. Zhang H, Jiao W, Cui H, Sun Q, Fan H. Combined exposure of alumina nanoparticles and chronic stress exacerbates hippocampal neuronal ferroptosis via activating IFN-gamma/ASK1/JNK signaling pathway in rats. *J Hazard Mater*. 2021;411:125179.
70. Amorim P, Telch B. A chemotaxis predator-prey model with indirect pursuit-evasion dynamics and parabolic signal. *J Math Anal Appl*. 2021. <https://doi.org/10.1016/j.jmaa.2021.125128>.
71. Melillo RM, Guarino V, Avilla E, Galdiero MR, Liotti F, Prevede N, Rossi FW, Basolo F, Ugolini C, de Paulis A, et al. Mast cells have a protumorigenic role in human thyroid cancer. *Oncogene*. 2010;29(47):6203–15.
72. Visciano C, Liotti F, Prevede N, Cali G, Franco R, Collina F, de Paulis A, Marone G, Santoro M, Melillo RM. Mast cells induce

epithelial-to-mesenchymal transition and stem cell features in human thyroid cancer cells through an IL-8-Akt-Slug pathway. *Oncogene*. 2015;34(40):5175–86.

73. Siiskonen H, Poukka M, Bykachev A, Tyynela-Korhonen K, Sironen R, Pasonen-Seppanen S, Harvima IT. Low numbers of tryptase(+) and chymase(+) mast cells associated with reduced survival and advanced tumor stage in melanoma. *Melanoma Res*. 2015;25(6):479–85.

### **Publisher's Note**

Springer Nature remains neutral with regard to jurisdictional claims in published maps and institutional affiliations.

**Ready to submit your research? Choose BMC and benefit from:**

- fast, convenient online submission
- thorough peer review by experienced researchers in your field
- rapid publication on acceptance
- support for research data, including large and complex data types
- gold Open Access which fosters wider collaboration and increased citations
- maximum visibility for your research: over 100M website views per year

**At BMC, research is always in progress.**

Learn more [biomedcentral.com/submissions](https://biomedcentral.com/submissions)

